Multiomic Characterization Reveals a Distinct Molecular Landscape in Young-Onset Pancreatic Cancer

Ifeanyichukwu Ogobuiro, MD, MHS[1]; Yasmine Baca, MS[2]; Jennifer R. Ribeiro, PhD[2]; Phillip Walker, PhD[2]; Gregory C. Wilson, MD[3]; Prateek Gulhati, MD, PhD[4]; John L. Marshall, MD[5]; Rachna T. Shroff, MD, MS[6]; David Spetzler, PhD, MBA[7]; Matthew J. Oberley, MD, PhD[7]; Daniel E. Abbott, MD[8]; Hong Jin Kim, MD[9]; David A. Kooby, MD[10]; Shishir K. Maithel, MD[10]; Syed A. Ahmad, MD[3]; Nipun B. Merchant, MD[1]; Joanne Xiu, PhD[2]; Peter J. Hosein, MD[11]; and Jashodeep Datta, MD[1]

DOI https://doi.org/10.1200/PO.23.00152

ABSTRACT

PURPOSE Using a real-world database with matched genomic-transcriptomic molecular data, we sought to characterize the distinct molecular correlates underlying clinical differences between patients with young-onset pancreatic cancer (YOPC; younger than 50 years) and patients with average-onset pancreatic cancer (AOPC; 70 years and older).

METHODS We analyzed matched whole-transcriptome and DNA sequencing data from 2,430 patient samples (YOPC, n = 292; AOPC, n = 2,138) from the Caris Life Sciences database (Phoenix, AZ). Immune deconvolution was performed using the quanTIseq pipeline. Overall survival (OS) data were obtained from insurance claims (n = 4,928); Kaplan-Meier estimates were calculated for age- and molecularly defined cohorts. Significance was determined as FDR-corrected *P* values (*Q*) < .05.

RESULTS Patients with YOPC had higher proportions of mismatch repair–deficient/microsatellite instability-high, *BRCA2*-mutant, and *PALB2*-mutant tumors compared with patients with AOPC, but fewer *SMAD4*-, *RNF43*-, *CDKN2A*-, and *SF3B1*-mutant tumors. Notably, patients with YOPC demonstrated significantly lower incidence of *KRAS* mutations compared with patients with AOPC (81.3% *v* 90.9%; *Q* = .004). In the *KRAS* wild-type subset (n = 227), YOPC tumors demonstrated fewer *TP53* mutations and were more likely driven by *NRG1* and *MET* fusions, whereas *BRAF* fusions were exclusively observed in patients with AOPC. Immune deconvolution revealed significant enrichment of natural killer cells, $CD8^+$ T cells, monocytes, and M2 macrophages in patients with YOPC relative to patients with AOPC, which corresponded with lower rates of *HLA-DPA1* homozygosity. There was an association with improved OS in patients with YOPC compared with patients with AOPC with *KRAS* wild-type tumors (median, 16.2 [YOPC-$KRAS^{WT}$] *v* 10.6 [AOPC-$KRAS^{WT}$] months; *P* = .008) but not *KRAS*-mutant tumors (*P* = .084).

CONCLUSION In this large, real-world multiomic characterization of age-stratified molecular differences in pancreatic ductal adenocarcinoma, YOPC is associated with a distinct molecular landscape that has prognostic and therapeutic implications.

ACCOMPANYING CONTENT

Appendix

Accepted August 25, 2023
Published November 9, 2023

JCO Precis Oncol 7:e2300152

INTRODUCTION

Pancreatic ductal adenocarcinoma (PDAC) is a highly lethal malignancy with a 5-year survival rate of 12%[1] and is a leading cause of cancer-related mortality in the United States.[2] PDAC is typically diagnosed in the seventh decade of life, referred to as average-onset pancreatic cancer (AOPC)[1,3]; however, young-onset pancreatic cancer (YOPC)—defined as diagnosis at age <50 years[4,5]—constitutes 6%-9% of newly detected PDAC and has steadily increased in incidence over the past two decades.[5-12] Emerging data indicate that smoking,[4,5] alcohol use,[13] obesity,[14] and family history[13,15,16] are risk factors for YOPC. YOPC also skews toward male sex[7,11] although rates in women—particularly Black women—are rising faster than in men.[6,7,12]

The heterogeneity in the molecular landscape of PDAC that underpins its broad range of tumor phenotypes is one of the driving forces for suboptimal outcomes

CONTEXT

Key Objective

Young-onset pancreatic cancer (YOPC) represents a growing proportion of patients diagnosed with pancreatic ductal adenocarcinoma before age 50 years, with distinct clinical characteristics. Using a large real-world molecular database, we characterized the molecular features underlying these clinical differences between patients with YOPC and patients with average-onset pancreatic cancer (AOPC; 70 years and older).

Knowledge Generated

Compared with AOPC, YOPC demonstrated an increased incidence of mutations in DNA repair genes such as *BRCA2* and *PALB2* but lower rates of alterations in oncogenic driver genes, most notably *KRAS.* Among the *KRAS* wild-type cohort, YOPC was more likely driven by *NRG1* and *MET* fusions, but not *BRAF* fusions. YOPC displayed enrichment of distinct immune cell subsets and had lower rates of *HLA-DPA1* homozygosity. Strikingly, patients with YOPC demonstrated improved overall survival that was restricted to the *KRAS* wild-type cohort.

Relevance

YOPC is associated with a distinct molecular and immune landscape that could inform targeted therapies for these patients.

despite modern multimodal therapy.[17] However, clinically annotated tumor profiling database studies such as the Know Your Tumor study have demonstrated that patients with PDAC experience longer survival when receiving therapies matching actionable mutations compared with nonmatched therapies.[18] Moreover, The Cancer Genome Atlas analysis of PDAC revealed that, excluding *KRAS* and *CDKN2A*, 42% of patients could be candidates for molecularly informed clinical trials.[19] The increasing armamentarium of precision medicine approaches for patients with PDAC emphasizes the critical need to understand tumor-level molecular differences between patients with YOPC and AOPC, which might inform personalized therapy in this subset of patients.

Efforts to describe molecular differences between YOPC and AOPC have been hampered by a lack of real-world, large-scale matched genomic and transcriptomic data, leading to conflicting conclusions between studies. For instance, Raffenne et al[3] found no substantial differences in the mutational landscape between patients with YOPC and AOPC, whereas others have identified higher *SMAD4* mutation rates, increased activation of the TGF-β pathway,[20] and differential expression of *CDKN2A* and *FOXC2* in YOPC compared with AOPC.[21] Despite these differences, some unifying signals have emerged, particularly that patients with YOPC harbor fewer oncogenic somatic *KRAS* mutations but more pathogenic germline mutations than patients with AOPC.[16,19,20] Further complicating our understanding of this question are the conflicting survival outcomes observed in these studies, with many indicating that patients with YOPC have improved survival,[9,11,22,23] but others showing either shorter or no difference in survival compared with patients with AOPC.[3,5,10,15,20,24] Together, these results illustrate gaps in our understanding of the genomic and transcriptomic correlates underlying clinical differences between patients with YOPC and AOPC.

In the present study, we analyzed a real-world multi-institutional cohort of 2,430 sequenced tumors—including 292 YOPC—to characterize the distinct molecular landscape associated with YOPC compared with AOPC and better understand molecular correlates underlying the divergent clinical outcomes in patients with YOPC.

METHODS

Patient Samples

Two thousand four hundred thirty histologically confirmed PDAC samples were identified in the Caris Life Sciences database (Phoenix, AZ) with matched DNA sequencing, whole-transcriptome sequencing (WTS), and immunohistochemistry (IHC) data. We stratified these specimens into YOPC (younger than 50 years at diagnosis; n = 292) and AOPC (70 years and older; n = 2,138). Among YOPCs, 179 were metastases and 113 were primary tumors; among AOPCs, 1,167 were metastases and 967 were primary tumors.

Next-Generation Sequencing

Tumor enrichment was achieved using manual microdissection of formalin-fixed, paraffin-embedded (FFPE) sections that were marked for areas with an at least 20% tumor content. Next-generation sequencing (NGS) was performed on genomic DNA using the NextSeq or NovaSeq 6000 platforms (Illumina, Inc, San Diego, CA). For NextSeq-sequenced tumors, a custom-designed SureSelect XT assay was used to enrich 592 whole-gene targets (Agilent

Technologies, Santa Clara, CA). For NovaSeq-sequenced tumors, a hybrid pull-down panel of baits designed to enrich for >700 clinically relevant genes at high coverage and read depth was used, along with a separate panel to enrich for an additional >20,000 genes at lower depth. Genetic variants were detected with >99% confidence and were categorized by board-certified molecular geneticists as previously described.[25] Tumor mutational burden (TMB)-high was defined as ≥10 mutations/Mb.

IHC

FFPE sections on glass slides were stained for PD-L1 (clone SP142 [Spring Bioscience, Pleasanton, CA]) using automated staining techniques, per the manufacturer's instructions, and were optimized and validated per Clinical Laboratory Improvement Amendments/College of American Pathologists and International Organization for Standardization requirements. Staining was identified as positive if its intensity on the membrane of the tumor cells was ≥2+ (on a semiquantitative scale of 0-3: 0 no staining, 1+ weak staining, 2+ moderate staining, or 3+ strong staining) and the percentage of positively stained cells was ≥5%.

Mismatch Repair Deficiency/Microsatellite Instability-High Status

Multiple test platforms were used to determine mismatch repair deficiency (dMMR)/microsatellite instability-high (MSI-H) status of the tumors profiled, including fragment analysis (FA, Promega, Madison, WI), IHC (MLH1, M1 antibody; MSH2, G2191129 antibody; MSH6, 44 antibody; and PMS2, EPR3947 antibody [Ventana Medical Systems, Tucson, AZ]), and NGS. The three platforms generated highly concordant results as previously reported[26]; in the rare cases of discordant results, dMMR/MSI-H status was determined in the order of IHC, FA, and NGS.

WTS

mRNA was isolated from manually microdissected areas of FFPE sections with a tumor content of at least 10%. Whole-transcriptome sequencing (WTS) was performed using the Illumina NovaSeq platform (Illumina, Inc, San Diego, CA) and the Agilent SureSelect Human All Exon V7 bait panel (Agilent Technologies, Santa Clara, CA); transcripts per million were reported. Gene fusions were detected using the ArcherDX fusion assay (ArcherDX, Boulder, CO) and Illumina MiSeq platform (Illumina MiSeq, San Diego, CA) as previously described.[27] Immune cell fractions were calculated from transcriptomic data using quanTIseq[28] and xCell.[29] Gene set enrichment analysis (GSEA) and Metascape pathway analysis were performed on WTS data.[30,31] HLA genotyping was performed using arcasHLA, an in silico tool that infers HLA genotypes from RNA sequencing data.[32] If a single HLA genotype was detected, the specimen was classified as homozygous, which can occur because of parental homozygosity or HLA loss of heterozygosity.

Statistical Analysis

Clinicodemographic features were compared using the chi-square test, with $P < .05$ considered statistically significant. Comparative analysis of molecular alterations in the cohorts was analyzed using chi-square or Fisher's exact tests. Tumor microenvironment cell fractions were analyzed among cohorts using nonparametric Kruskal-Wallis testing. Because these closely related cohorts are only differentiated by age, P values of < .05 were highlighted as relevant trends. For a more stringent analysis of the differences between AOPC and YOPC, P values were corrected for multiple hypothesis testing using the Benjamini-Hochberg method to avoid type I error and adjusted $Q < .05$ was considered statistically significant.

Clinical Outcomes Data

Real-world overall survival (OS) information was obtained from insurance claims data and calculated from the date of tissue collection to last contact. Kaplan-Meier estimates were calculated for YOPC and AOPC in the entire cohort of patients with clinical data in the Caris CODEai clinicogenomic database (n = 4,928) and stratified by *KRAS* mutation status (n = 3,116 patients with *KRAS* data; $KRAS^{WT}$, n = 393; $KRAS^{MUT}$, n = 2,723); these numbers differ from the molecular analysis since the database is constantly increasing in size. Significance was determined as log-rank $P < .05$.

Compliance Statement

This study was approved by the Institutional Review Board at the University of Miami and conducted in accordance with guidelines of the Declaration of Helsinki, Belmont report, and US Common rule. Per 45 CFR 46.101(b)(4), this study used retrospective, deidentified clinical data and no patient consent was necessary from the patients.

Data Availability

Data presented in this study are not publicly available because of data size and patient privacy but are available on reasonable request from the corresponding author.

RESULTS

Clinicodemographic Characteristics

At the time of molecular analysis, 2,430 patient samples were annotated with genomic and transcriptomic data. A total of 4,928 patients had available clinical outcomes data in the most recent query of the Caris CODEai clinicogenomic database, from which Kaplan-Meier curves were generated.

TABLE 1. Clinicodemographic Characteristics of Patients With PDAC From the Caris Life Sciences Database

Variable	YOPC, No. (%)	AOPC, No. (%)	*P*
Median age (years)	46	75	
Sex			<.05
Male	190 (65)	1,116 (52)	
Female	102 (35)	1,022 (48)	
Smoking status			.023
Current	18 (95)	142 (91)	
Nonsmoker	1 (5)	14 (9)	

NOTE. Specimens were stratified by YOPC and AOPC and analyzed by sex and smoking status. *P* values were determined by Fisher's exact test.
Abbreviations: AOPC, average-onset pancreatic cancer; PDAC, pancreatic ductal adenocarcinoma; YOPC, young-onset pancreatic cancer.

Of the 2,430 patients with molecular data, 292 patients (12%) had YOPC, with the median age being 46 years (IQR, 41-48). Among 2,138 patients with AOPC (88%), the median age was 75 years (IQR, 72-79). There was a significant preponderance of male patients (65% *v* 52%; $P < .05$) and current smokers (95% *v* 91%; $P = .023$) in patients with YOPC compared with patients with AOPC, respectively (Table 1).

Comparative Molecular Landscape of YOPC and AOPC

Previous studies have reported differing prevalence of molecular alterations[3,19,20,33,34] and a preponderance of germline mutations in *BRCA1/2* and MMR genes in patients with YOPC compared with patients with AOPC.[16] However, direct comparisons between YOPC and AOPC are scarce and have used smaller cohorts.[3,20] We analyzed clinically relevant pathogenic/likely pathogenic mutations and copy number alterations in tumors from patients with YOPC and AOPC from this real-world cohort (Appendix Table A1).

KRAS mutations were the most prevalent somatic alterations in both YOPC and AOPC (81.3% and 90.9%), followed by *TP53* (69.3% and 74.7%), *CDKN2A* (19.3% and 24.8%), and *SMAD4* (14.7% and 20.1%; Figs 1A and 1B), respectively. Although germline mutational data were unavailable, patients with YOPC had significantly higher rates of alterations in homologous recombination repair (HRR) genes detected in their tumors, specifically *BRCA2* (4.7% *v* 2.1%; $P = .008$) and *PALB2* (1.4% *v* 0.5%; $P = .044$), compared with patients with AOPC. Patients with YOPC were also noted to have higher rates of dMMR/MSI-H tumors (2.8% *v* 0.8%; $P = .001$) compared with patients with AOPC.

Conversely, patients with AOPC had significantly higher rates of oncogenic *KRAS* mutations compared with patients with YOPC (90.9% *v* 81.3%; $P = 1.10e-6$; $Q = .004$) and significantly higher rates of alterations in *CDKN2A* (24.8% *v* 19.25%; $P = .045$), *SMAD4* (20.1% *v* 14.7%; $P = .033$), *RNF43* (6.3% *v* 2.5%; $P = .012$), and *SF3B1* (2.7% *v* 0.7%; $P = .046$; Figs 1A and 1B).

Spectrum of Alterations Within *KRAS*^{WT} Tumors in Patients With YOPC and AOPC

We next dissected the landscape of molecular alterations within the *KRAS* wild-type (*KRAS*^{WT}; n = 227 [10.7%]) cohort, given the significant enrichment of *KRAS*^{WT} tumors in patients with YOPC (Fig 2A). Previous studies have implicated the enrichment of mutations in *BRAF*, *CTNNB1*, and alternative RAS pathway genes[19] in *KRAS*^{WT} PDAC. Accordingly, we observed trends toward increased rates of *CTNNB1* mutations (17.7% *v* 4.0%; $P = .002$) and reduced rates of pathogenic *TP53* mutations (21.3% *v* 44.4%; $P = .004$) in YOPC-*KRAS*^{WT} tumors compared with AOPC-*KRAS*^{WT} tumors. Moreover, YOPC-*KRAS*^{WT} patients demonstrated higher rates of *MET* (4.1% *v* 0.6%; $P = .12$) and *NRG1* (6.1% *v* 1.1%; $P = .07$) fusions compared with AOPC-*KRAS*^{WT} patients, whereas *BRAF* fusions were exclusively concentrated in AOPC-*KRAS*^{WT} compared with YOPC-*KRAS*^{WT} tumors (6.8% *v* 0.0%; $P = .07$; Fig 2B). These results indicate distinct molecular vulnerabilities in *KRAS*^{WT} tumors when stratifying by age of PDAC onset.

Differentially Regulated Signaling Pathways in Tumor Transcriptomes From Patients With YOPC Versus AOPC

To better understand how these genomic differences between YOPC and AOPC tumors influence downstream oncogenic and tumor microenvironment signaling, we performed GSEA comparing whole-tumor transcriptomes in YOPC versus AOPC. A relatively narrow number—that is, total of 20—of genes were significantly differentially expressed ($P < .05$; $Q < .25$) between YOPC and AOPC (Fig 3A; Appendix Table A2). The top genes more highly expressed in YOPC included carboxypeptidase B (*CPB2*), plasminogen (*PLG*), prothrombin (*F2*), and genes for fibrinogen alpha and beta chains (*FGA/FGB*), whereas plasminogen activator inhibitor 2 (*SERPINB2*) and interferon gamma (*IFNG*) had significantly higher expression in AOPC. We then used a less stringent *P* value cutoff ($P < .25$) in Metascape pathway analysis to clarify the transcriptomic nuances of these age-stratified PDAC cohorts. This analysis revealed that YOPC tumor transcriptomes were significantly enriched in pathways related to blood clotting cascade, extracellular matrix, cancer pathways, cytokine/inflammatory response, and angiogenesis (Fig 3B).

Intratumoral Immune Deconvolution and HLA Landscape in YOPC Versus AOPC

Because of the enrichment of select pathways and somatic alterations with diverse immunologic repercussions in YOPC, we sought to determine differences in the tumor immune microenvironment between YOPC and AOPC

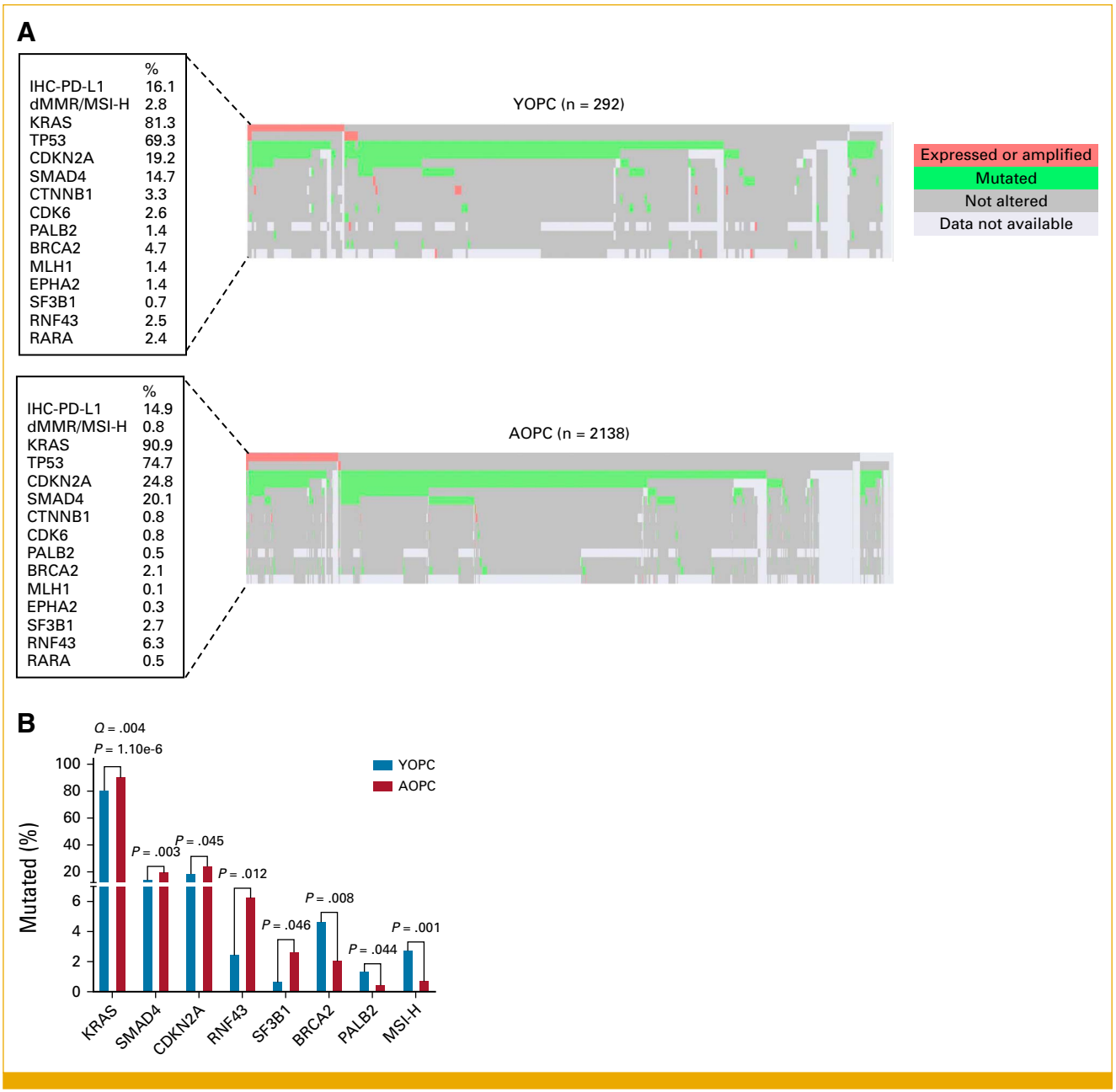

FIG 1. Molecular landscape of YOPC and AOPC. (A) Oncoprints displaying the pathogenic molecular alteration pattern of YOPC (n = 292) and AOPC (n = 2,138). Columns represent tumor samples. Rows represent individual molecular biomarkers, whose percentages in the cohort are described in the boxes to the left of oncoprints. Pink, expressed or amplified; green, mutated; gray; not altered; light gray, data not available. (B) Bar graph showing statistically significant differential molecular alterations in YOPC (blue bars, n = 292) versus AOPC (red bars, n = 2,138). *P* values (chi-square or Fisher's exact tests) and FDR-adjusted *Q* values are indicated above the compared groups for each molecular alteration. AOPC, average-onset pancreatic cancer; FDR, false discovery rate; YOPC, young-onset pancreatic cancer.

using quanTIseq immune deconvolution.[28] While there were no significant differences in rates of TMB-high tumors, PD-L1 positivity (via IHC), or immune checkpoint gene expression between the cohorts (Appendix Figs A1A and A1B), there was a statistically significant enrichment in computationally inferred signatures for natural killer (NK) cells (P = .009; Q = .039), CD8$^+$ T cells (P = .043; Q = .117), M2 macrophages (P = .011; Q = .039), and monocytic cells (P = .002; Q = .021) in tumors from patients with YOPC compared with AOPC (Figs 4A and 4B). We then used xCell deconvolution[29] to further compare CD8$^+$ T-cell subsets between cohorts, which revealed no differences in effector or central memory CD8$^+$ T cells but demonstrated enrichment of naïve CD8$^+$ T cells in tumors from patients with YOPC (Appendix Fig A1C).

To further understand potential major histocompatibility complex determinants that might underlie these

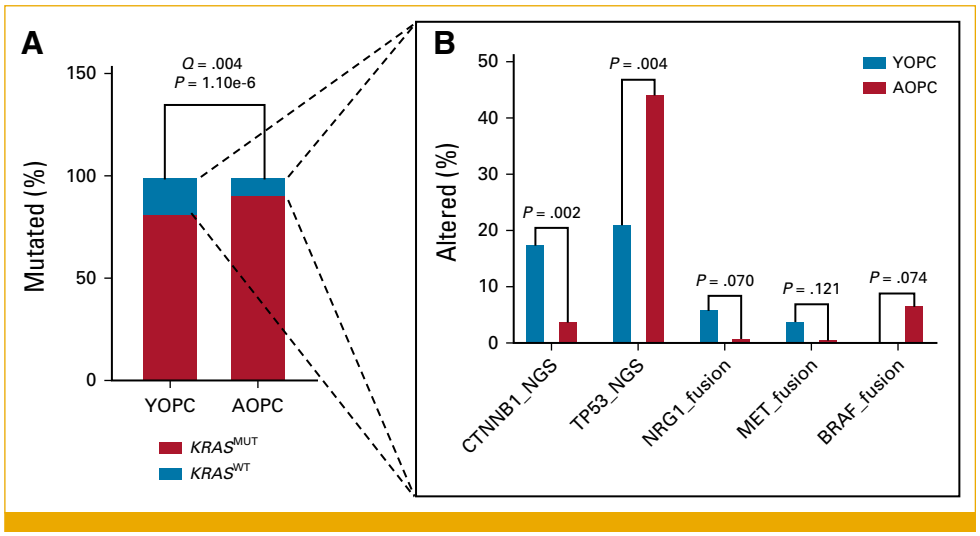

FIG 2. Spectrum of alterations within *KRAS* wild-type YOPC and AOPC tumors. (A) Frequency of *KRAS* wild-type (*KRAS*^{WT}; blue, n = 227) and *KRAS*-mutant (*KRAS*^{MUT}; red, n = 1,970) tumors in YOPC and AOPC, determined by next-generation sequencing for pathogenic alterations. (B) *KRAS*^{WT} tumors, indicated in blue in (A), were analyzed separately for differences in pathogenic molecular alterations. The spectrum of top mutations and fusions within *KRAS*^{WT} YOPC (blue bars, n = 49-51 [two YOPC-*KRAS*^{WT} patients lacked WTS data for fusions]) and AOPC (red bars, n = 176) is shown, with *P* values (chi-square or Fisher's exact tests) indicated. AOPC, average-onset pancreatic cancer; WTS, whole transcriptome sequencing; YOPC, young-onset pancreatic cancer.

immunologic differences between cohorts, we examined HLA-type and locus-specific expression inferred from RNA sequencing data. We observed a significantly decreased rate of homozygosity in *HLA-DPA1* in tumors from patients with YOPC compared with AOPC (55.2% *v* 64.1%; $P = .003$; $Q = .026$; Fig 4C). Taken together, these associative data illustrate potential differences in immunogenicity related to cell-autonomous and/or non-autonomous mediators in tumors from patients with YOPC that might be contributory to differences in clinicopathologic outcomes between patients with YOPC and AOPC.

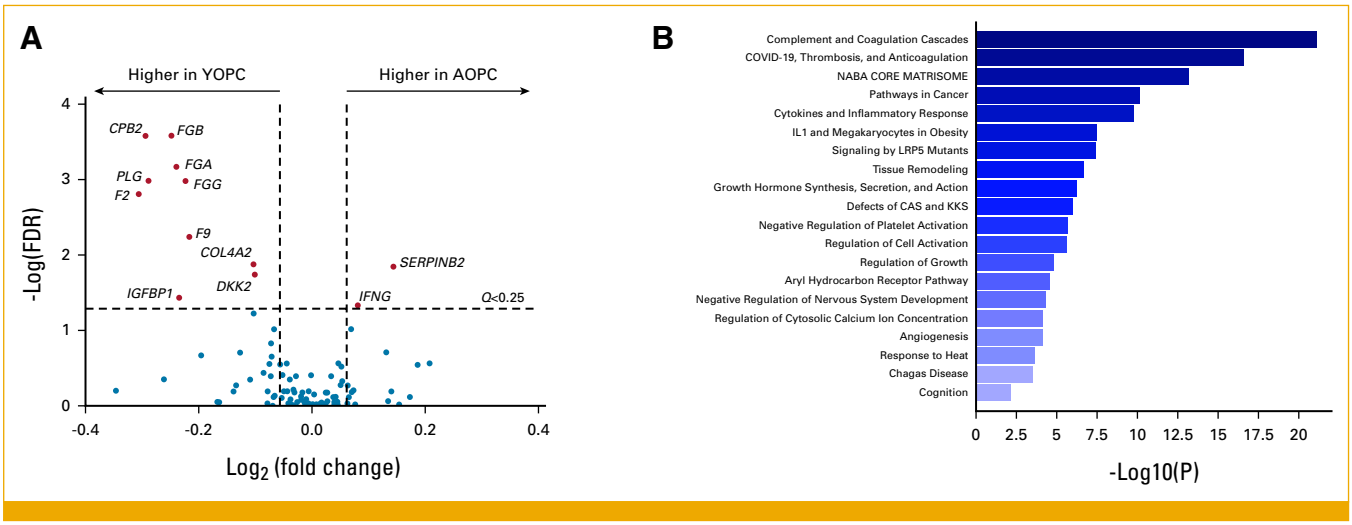

FIG 3. Differentially regulated signaling pathways in YOPC and AOPC. (A) The volcano plot shows DEGs between YOPC (n = 284) and AOPC (n = 2,089), with a cutoff of FDR-adjusted $Q < .25$. Genes to the left indicated in red are significantly higher in YOPC, whereas genes to the right indicated in red are significantly higher in AOPC. (B) Metascape pathway enrichment analysis was performed on 40 DEGs between YOPC and AOPC ($P < .25$). The bar graph indicates canonical signaling pathways and biologic processes differentially enriched in the tumor transcriptomes of YOPC compared with AOPC tumor samples. The *x*-axis indicates statistical significance ($-\log_{10}$ *P* value). AOPC, average-onset pancreatic cancer; CAS, contact activation system; DEGs, differentially expressed genes; FDR, false discovery rate; KKS, kallikrein/kinin system; YOPC, young-onset pancreatic cancer.

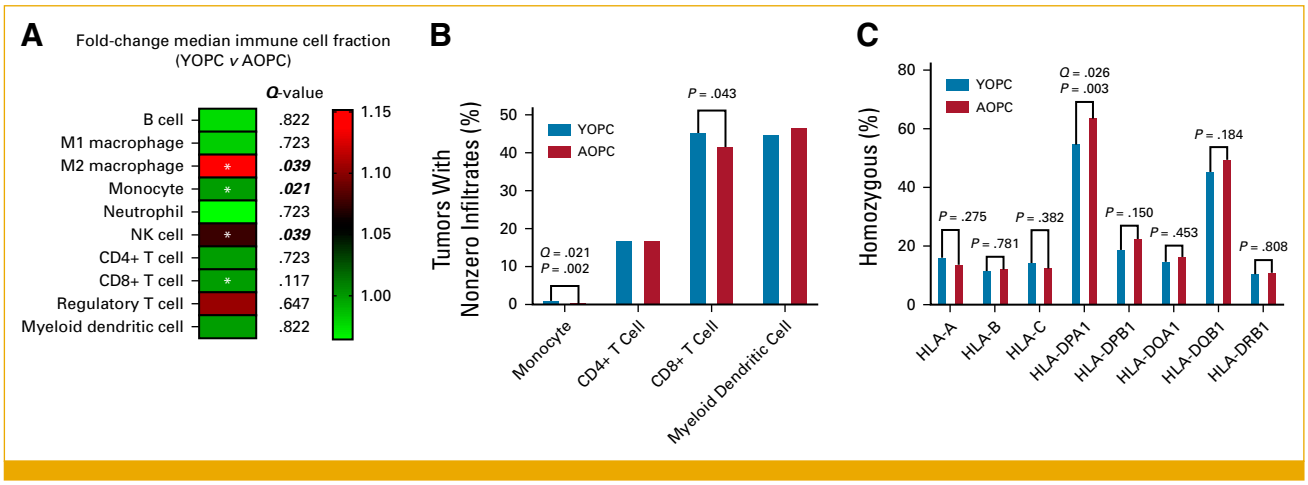

FIG 4. Intratumoral immune populations and HLA landscape in YOPC and AOPC. (A) Computationally inferred intratumoral immune population between YOPC (n = 284) and AOPC (n = 2,089). The heatmap indicates fold change (YOPC *v* AOPC) in median immune fraction according to quanTIseq. *P* values were determined using the nonparametric Kruskal-Wallis test. Asterisks indicate $P < .05$, with *Q* values shown to the right. Italicized/bolded *Q* values indicate $Q < .05$. (B) For cell types with median values of "0" (ie, monocytes, $CD4^+$ T cells, $CD8^+$ T cells, and myeloid dendritic cells), the percentage of tumors with nonzero immune infiltrates were compared. (C) Differences in HLA landscape inferred from WTS data in YOPC (blue bars, n = 284) compared with AOPC (red bars, n = 2,089). *P* values (chi-square or Fisher's exact test) and FDR-adjusted *Q* values are indicated above compared groups for each HLA gene. AOPC, average-onset pancreatic cancer; FDR, false discovery rate; WTS, whole-transcriptome sequencing; YOPC, young-onset pancreatic cancer.

OS of Patients With YOPC and AOPC Stratified by *KRAS*^{MUT} and *KRAS*^{WT}

The Caris CODEai data set included 4,928 patients with insurance claims–related follow-up information, but limited clinicopathologic data precluded stage- and treatment-stratified comparisons between YOPC and AOPC cohorts. Notwithstanding, we observed significantly longer OS in patients with YOPC compared with patients with AOPC (14.9 *v* 10.8 months; $P < .00001$; Fig 5A). Given the differences in frequency of *KRAS*-altered tumors between cohorts, we further analyzed the effect of *KRAS* alteration status on OS. YOPC-*KRAS*^{WT} patients had significantly prolonged OS compared with AOPC-*KRAS*^{WT} patients (16.2 *v* 10.6 months; $P = .008$; Fig 5B). However, there was no difference in OS between patients with YOPC and AOPC with *KRAS*^{MUT} tumors (12.9 *v* 10.0 months; $P = .084$; Fig 5C). These data suggest that survival differences between patients with YOPC and AOPC in the overall cohort may be driven by survival variation specifically in patients harboring *KRAS*^{WT} tumors.

DISCUSSION

To our knowledge, the present study represents the largest pragmatic molecular comparison of YOPC versus AOPC. Our data reinforce previously observed epidemiologic distinctions between patients with YOPC and AOPC,[4,5,7,11] specifically its male preponderance and association with active smoking behaviors in patients with YOPC, and conclusively reveal a higher incidence of *KRAS*^{WT} tumors in YOPC. Within this *KRAS*^{WT} subset, we uncovered distinct molecular vulnerabilities when stratifying by age—that is, *MET* and *NRG1* fusions in YOPC-*KRAS*^{WT} and *BRAF* fusions in AOPC-*KRAS*^{WT}. Among the unstratified cohort, tumors from patients with YOPC demonstrated higher rates of alterations in HRR genes, higher prevalence of dMMR/MSI-H, and enrichment of NK cells and naïve $CD8^+$ T cells. Finally, our data reconcile conflicting previous evidence by demonstrating improved survival in patients with YOPC compared with patients with AOPC, which may not only reflect the reduced prevalence of the virulent oncogenic drivers *KRAS*, *SMAD4*, and *CDKN2A* in tumor genomes of YOPC patients but also be driven by the significantly longer survival of YOPC-*KRAS*^{WT} versus AOPC-*KRAS*^{WT} patients.

While the success of targeted and immune-based therapies has significantly lagged in PDAC compared with other solid tumors, the Know Your Tumor study illustrated the oncologic importance of molecularly matched targeted therapies in patients with advanced PDAC.[18] To that end, our data provide a biologic map of the distinct molecular vulnerabilities in patients with YOPC that might be exploited therapeutically. While *KRAS* mutations—with their rapidly evolving therapeutic landscape—[35,36]are ubiquitous in the broader cohort, our data reveal novel age-restricted molecular alterations in *KRAS*^{WT} tumors that may be clinically actionable; *NRG1*, *MET*, and *BRAF* fusions each have associated targeted therapies (eg, afatinib, capmatinib, and encorafenib/vemurafenib, respectively).[37-39] Moreover, given recent data indicating the benefit of polyADP-ribose polymerase inhibitors (PARPi) in patients with germline or somatic mutations in HRR genes,[40] the enrichment of *BRCA2* and *PALB2* alterations in YOPC tumors suggests that a higher proportion of patients with YOPC may ultimately

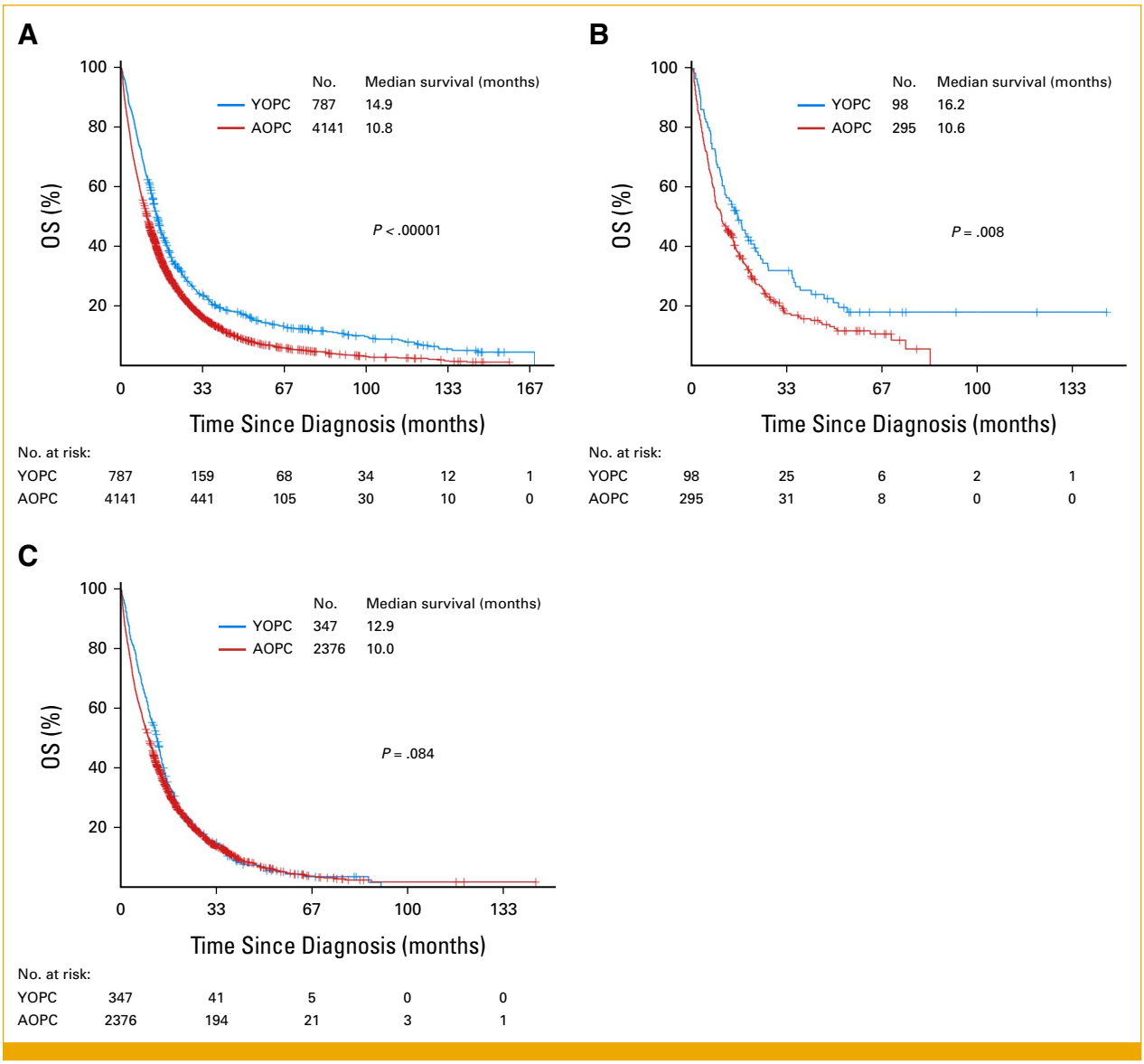

FIG 5. OS of patients with YOPC and AOPC stratified by *KRAS*^{MUT} and *KRAS*^{WT}. (A) Kaplan-Meier curves depict the OS of patients with YOPC (blue line, n = 787) versus patients with AOPC (red line, n = 2,753) in the entire PDAC cohort with clinical outcome data (n = 4,141 total). (B) and (C) All PDAC cases with *KRAS* mutation data available were stratified by *KRAS* status. Kaplan-Meier curves depict the OS of patients with YOPC (blue line, n = 98) versus patients with AOPC (red line, n = 295) with *KRAS*^{WT} tumors (n = 393 total; B) and patients with YOPC (blue line, n = 347) and AOPC (red line, n = 2,376) *KRAS*^{MUT} tumors (n = 2,723 total; C). AOPC, average-onset pancreatic cancer; OS, overall survival; PDAC, pancreatic ductal adenocarcinoma; YOPC, young-onset pancreatic cancer.

be eligible for PARPi. Taken together, these data call for heightened awareness among clinician and nonclinician stakeholders of the distinct genomic landscape in patients with YOPC and underscore the importance of routine NGS testing in younger patients presenting with newly diagnosed advanced PDAC to inform potential molecularly targeted therapeutic approaches.

Exploration of the transcriptomes differentially expressed between YOPC and AOPC revealed enrichment of pathways associated with thrombotic cascades, extracellular matrix, cancer pathways, and cytokine/inflammatory response, which suggests possible restriction of tumor immunity in YOPC.[41-43] Conversely, the significant reduction in *HLA-DPA1* homozygosity—which has been previously associated with dampened antigen presentation and checkpoint blockade efficacy[44]—and associated increases in computationally inferred adaptive immune subpopulations (ie, NK and CD8^{+} T cells) in YOPC suggest a less immunosuppressive and more immunostimulatory microenvironment. While the impact of greater numbers of intratumoral naïve CD8^{+} T cells in YOPC is unclear, higher circulating levels of these cells have been associated with improved prognosis in other solid tumors, for example, non–small-cell lung

cancer.[45] These findings underscore the need for deeper investigation and functional characterization of cell-autonomous and nonautonomous immunologic repercussions in YOPC tumors. The differentially expressed transcriptome we observed in patients with YOPC in the current study, however, is not strongly consistent with previous—albeit underpowered—studies that revealed enrichment in pathways predominantly related to hedgehog signaling and hypoxia in YOPC.[3,20] This lack of concordance might be attributable to our substantially larger cohort size and/or the inherent heterogeneity of patients enrolled in this pragmatic real-world study capturing data with wide geographic and clinicodemographic variability, which present novel insights into the genotype-immunophenotype chasm in YOPC.[46]

Our study has several limitations. First, while the classification of YOPC and AOPC into age cutoffs of <50 and ≥70-year was informed in previous studies,[3-5] this arbitrary distinction may underestimate subtle molecular differences in patients with YOPC. Second, while several of the reported genomic differences did not achieve significance by multiple hypothesis testing, we felt it important to report these novel signals with the recognition that our study compares molecular determinants in two closely related PDAC patient populations differentiated solely by a 20-year age gap. Further validation of the subtle molecular features distinguishing these cohorts is warranted. Third, the lack of clinical annotation (eg, performance status, resection status, stage, BMI, and multimodality treatment information) in the Caris CODEai data set precluded our ability to perform multivariable analyses to account for confounding by these clinical parameters.

Given the rise in YOPC diagnosis in recent years,[5-11] these data are a timely addition to an expanding compendium of molecular taxonomy that highlights the clinical and phenotypic heterogeneities observed in this distinct cohort of patients.[4,5,7,11,16,19-21] Furthermore, novel genomic and transcriptomic signals observed in tumors from patients with YOPC may offer a putative molecular basis for the divergent clinical outcomes observed in this population. Moving forward, these data could be incorporated into future trial design to allow more precise selection and stratification of patients with YOPC and AOPC for elements of multimodality and/or novel therapies, with the goal of improving contemporary survival outcomes in this lethal malignancy.

AFFILIATIONS

[1]Department of Surgery, Sylvester Comprehensive Cancer Center, University of Miami Leonard M. Miller School of Medicine, Miami, FL
[2]Caris Life Sciences, Phoenix, AZ
[3]University of Cincinnati Medical Center, Cincinnati, OH
[4]Robert Wood Johnson Medical School, The Cancer Institute of NJ, New Brunswick, NJ
[5]Georgetown University, Washington, DC
[6]University of Arizona Cancer Center, Tucson, AZ
[7]Caris Life Sciences, Irving, TX
[8]University of Wisconsin Carbone Cancer Center, Madison, WI
[9]The University of North Carolina at Chapel Hill, Chapel Hill, NC
[10]Winship Cancer Institute, Emory University, Atlanta, GA
[11]Department of Medicine, University of Miami Leonard M. Miller School of Medicine, Miami, FL

PREPRINT VERSION

Preprint version available on medRxiv (https://www.medrxiv.org/node/634311.full).

CORRESPONDING AUTHOR

Jashodeep Datta, MD, Division of Surgical Oncology, Department of Surgery, Sylvester Comprehensive Cancer Center, University of Miami Miller School of Medicine, 1120 NW 14th St, Ste 410, Miami, FL 33136; e-mail: jash.datta@med.miami.edu.

PRIOR PRESENTATION

Presented in part at the ASCO Gastrointestinal Cancers Symposium Annual Meeting, San Francisco, CA, January 20-22, 2022 and the Society of Surgical Oncology Annual Meeting, Dallas, TX, March 9-12, 2022.

SUPPORT

Supported by KL2 career development grant from the Miami Clinical and Translational Science Institute under National Institutes of Health (NIH) Award UL1TR002736, American College of Surgeons Franklin H. Martin Research Fellowship, Association for Academic Surgery Joel J. Roslyn Faculty Award, Society of Surgical Oncology Young Investigator Award, and Elsa U. Pardee Foundation Award (to J.D.). I.O. was supported by NIH/National Cancer Institute (NCI) T32 (to N.B.M.). Research reported in this publication was supported by the NCI/NIH Award P30CA240139 to the Sylvester Comprehensive Cancer Center.

AUTHOR CONTRIBUTIONS

Conception and design: Ifeanyichukwu Ogobuiro, Gregory C. Wilson, John L. Marshall, Hong Jin Kim, David A. Kooby, Shishir K. Maithel, Syed A. Ahmad, Nipun B. Merchant, Joanne Xiu, Peter J. Hosein, Jashodeep Datta
Financial support: Nipun B. Merchant, Joanne Xiu, Jashodeep Datta
Administrative support: Nipun B. Merchant, Joanne Xiu, Jashodeep Datta
Provision of study materials or patients: Matthew J. Oberley, Hong Jin Kim, Syed A. Ahmad, Nipun B. Merchant, Joanne Xiu, Jashodeep Datta
Collection and assembly of data: Ifeanyichukwu Ogobuiro, Jennifer R. Ribeiro, Rachna T. Shroff, David Spetzler, Matthew J. Oberley, Shishir K. Maithel, Joanne Xiu, Peter J. Hosein, Jashodeep Datta
Data analysis and interpretation: Ifeanyichukwu Ogobuiro, Yasmine Baca, Phillip Walker, Gregory C. Wilson, Prateek Gulhati, John L. Marshall, Rachna T. Shroff, Matthew J. Oberley, Daniel E. Abbott, Hong Jin Kim, Shishir K. Maithel, Syed A. Ahmad, Nipun B. Merchant, Joanne Xiu, Peter J. Hosein, Jashodeep Datta
Manuscript writing: All authors
Final approval of manuscript: All authors
Accountable for all aspects of the work: All authors

AUTHORS' DISCLOSURES OF POTENTIAL CONFLICTS OF INTEREST

The following represents disclosure information provided by authors of this manuscript. All relationships are considered compensated unless otherwise noted. Relationships are self-held unless noted.
I = Immediate Family Member, Inst = My Institution. Relationships may not relate to the subject matter of this manuscript. For more information about ASCO's conflict of interest policy, please refer to www.asco.org/rwc or ascopubs.org/po/author-center.
Open Payments is a public database containing information reported by companies about payments made to US-licensed physicians (Open Payments).

Yasmine Baca
Employment: Caris Life Sciences

Jennifer R. Ribeiro
Employment: Caris Life Sciences
Stock and Other Ownership Interests: Caris Life Sciences

Phillip Walker
Employment: Caris Life Sciences

John L. Marshall
Employment: Caris Life Sciences, Indivumed
Leadership: 2curex
Honoraria: Bayer/Onyx, Taiho Pharmaceutical, Caris Life Sciences, Merck, Pfizer, Daiichi Sankyo/Lilly, AstraZeneca/MedImmune, Seagan
Consulting or Advisory Role: Genentech/Roche, Taiho Pharmaceutical, Caris Life Sciences, Pfizer, Seagen, Merck, AstraZeneca
Speakers' Bureau: Taiho Pharmaceutical, Merck, Pfizer, Seagan, Caris Life Sciences
Research Funding: Genentech, Natera

Rachna T. Shroff
Consulting or Advisory Role: Exelixis, Merck, Incyte, AstraZeneca, Taiho Pharmaceutical, Boehringer Ingelheim, Genentech, Jazz Pharmaceuticals, Merus
Research Funding: Merck, Exelixis, QED Therapeutics, Rafael Pharmaceuticals, Bristol Myers Squibb, Bayer, Immunovaccine, Seagen, Novocure, Nucana, Loxo/Lilly, Faeth Therapeutics, NGM Biopharmaceuticals, Actuate Therapeutics

David Spetzler
Employment: Caris Life Sciences
Stock and Other Ownership Interests: Caris Life Sciences
Honoraria: Caris Life Sciences
Research Funding: Caris Life Sciences
Patents, Royalties, Other Intellectual Property: Caris Life Sciences holds and has pending patents with intellectual property interests relating to health and medicine
Travel, Accommodations, Expenses: Caris Life Sciences

Matthew J. Oberley
Employment: Caris Life Sciences
Leadership: Caris Life Sciences
Stock and Other Ownership Interests: Caris Life Sciences
Travel, Accommodations, Expenses: Caris Life Sciences

Daniel E. Abbott
Honoraria: Castle Biosciences
Consulting or Advisory Role: PatientPoint

Hong Jin Kim
Consulting or Advisory Role: Ethicon

David A. Kooby
Consulting or Advisory Role: Medtronic

Shishir K. Maithel
Consulting or Advisory Role: AstraZeneca
Research Funding: Celgene

Syed A. Ahmad
Speakers' Bureau: AbbVie

Nipun B. Merchant
Stock and Other Ownership Interests: Singh Molecular Medicine, LLC
Research Funding: Swedish Orphan Biovitrum AG

Joanne Xiu
Employment: Caris Life Sciences

Peter J. Hosein
Honoraria: AngioDynamics
Research Funding: Eisai (Inst)
Open Payments Link: https://openpaymentsdata.cms.gov/physician/1108197

No other potential conflicts of interest were reported.

REFERENCES

1. Siegel RL, Miller KD, Fuchs HE, et al: Cancer statistics, 2022. CA Cancer J Clin 72:7-33, 2022
2. Rahib L, Smith BD, Aizenberg R, et al: Projecting cancer incidence and deaths to 2030: The unexpected burden of thyroid, liver, and pancreas cancers in the United States. Cancer Res 74: 2913-2921, 2014
3. Raffenne J, Martin FA, Nicolle R, et al: Pancreatic ductal adenocarcinoma arising in young and old patients displays similar molecular features. Cancers (Basel) 13:1234, 2021
4. Raimondi S, Maisonneuve P, Löhr JM, et al: Early onset pancreatic cancer: Evidence of a major role for smoking and genetic factors. Cancer Epidemiol Biomarkers Prev 16:1894-1897, 2007
5. Piciucchi M, Capurso G, Valente R, et al: Early onset pancreatic cancer: Risk factors, presentation and outcome. Pancreatology 15:151-155, 2015
6. Tavakkoli A, Singal AG, Waljee AK, et al: Racial disparities and trends in pancreatic cancer incidence and mortality in the United States. Clin Gastroenterol Hepatol 18:171-178.e10, 2020
7. LaPelusa M, Shen C, Arhin ND, et al: Trends in the incidence and treatment of early-onset pancreatic cancer. Cancers (Basel) 14:283, 2022
8. Tingstedt B, Weitkämper C, Andersson R: Early onset pancreatic cancer: A controlled trial. Ann Gastroenterol 24:206-212, 2011
9. Beeghly-Fadiel A, Luu HN, Du L, et al: Early onset pancreatic malignancies: Clinical characteristics and survival associations. Int J Cancer 139:2169-2177, 2016
10. Ansari D, Althini C, Ohlsson H, et al: Early-onset pancreatic cancer: A population-based study using the SEER registry. Langenbecks Arch Surg 404:565-571, 2019
11. Saadat LV, Chou JF, Gonen M, et al: Treatment patterns and survival in patients with early-onset pancreatic cancer. Cancer 127:3566-3578, 2021
12. The Lancet Gastroenterology Hepatology: Cause for concern: The rising incidence of early-onset pancreatic cancer. Lancet Gastroenterol Hepatol 8:287, 2023
13. Bunduc S, Iacob R, Costache R, et al: Very early onset pancreatic adenocarcinoma—Clinical presentation, risk factors and therapeutic options. Chirurgia (Bucur) 113:405-411, 2018
14. Saeed U, Myklebust T, Robsahm TE, et al: Body mass index and pancreatic adenocarcinoma: A nationwide registry-based cohort study. Scand J Surg 112:11-21, 2023
15. Ulanja MB, Moody AE, Beutler BD, et al: Early-onset pancreatic cancer: A review of molecular mechanisms, management, and survival. Oncotarget 13:828-841, 2022
16. Bannon SA, Montiel MF, Goldsein JB, et al: High prevalence of hereditary cancer syndromes and outcomes in adults with early-onset pancreatic cancer. Cancer Prev Res (Phila) 11:679-686, 2018
17. DeSantis CE, Lin CC, Mariotto AB, et al: Cancer treatment and survivorship statistics, 2014. CA Cancer J Clin 64:252-271, 2014
18. Pishvaian MJ, Blais EM, Brody JR, et al: Overall survival in patients with pancreatic cancer receiving matched therapies following molecular profiling: A retrospective analysis of the Know Your Tumor registry trial. Lancet Oncol 21:508-518, 2020
19. Raphael BJ, Hruban RH, Aguirre AJ, et al: Integrated genomic characterization of pancreatic ductal adenocarcinoma. Cancer Cell 32:185-203.e13, 2017
20. Ben-Aharon I, Elkabets M, Pelossof R, et al: Genomic landscape of pancreatic adenocarcinoma in younger versus older patients: Does age matter? Clin Cancer Res 25:2185-2193, 2019
21. Lou E: Age is in the eye of the beholder: Distinguishing molecular signatures in early-onset pancreatic adenocarcinomas. Clin Cancer Res 27:8-10, 2021
22. Luo J, Xiao L, Wu C, et al: The incidence and survival rate of population-based pancreatic cancer patients: Shanghai Cancer Registry 2004-2009. PloS One 8:e76052, 2013
23. He J, Edil BH, Cameron JL, et al: Young patients undergoing resection of pancreatic cancer fare better than their older counterparts. J Gastrointest Surg 17:339-344, 2013

24. Ntala C, Debernardi S, Feakins RM, et al: Demographic, clinical, and pathological features of early onset pancreatic cancer patients. BMC Gastroenterol 18:139, 2018
25. Shaikh H, McGrath JE, Hughes B, et al: Genomic and molecular profiling of human papillomavirus associated head and neck squamous cell carcinoma treated with immune checkpoint blockade compared to survival outcomes. Cancers (Basel) 13:6309, 2021
26. Vanderwalde A, Spetzler D, Xiao N, et al: Microsatellite instability status determined by next-generation sequencing and compared with PD-L1 and tumor mutational burden in 11,348 patients. Cancer Med 7:746-756, 2018
27. Ferguson SD, Zhou S, Huse JT, et al: Targetable gene fusions associate with the IDH wild-type astrocytic lineage in adult gliomas. J Neuropathol Exp Neurol 77:437-442, 2018
28. Finotello F, Mayer C, Plattner C, et al: Molecular and pharmacological modulators of the tumor immune contexture revealed by deconvolution of RNA-seq data. Genome Med 11:34, 2019
29. Aran D, Hu Z, Butte AJ: xCell: digitally portraying the tissue cellular heterogeneity landscape. Genome Biol 18:220, 2017
30. Zhou Y, Zhou B, Pache L, et al: Metascape provides a biologist-oriented resource for the analysis of systems-level datasets. Nat Commun 10:1523, 2019
31. Subramanian A, Tamayo P, Mootha VK, et al: Gene set enrichment analysis: A knowledge-based approach for interpreting genome-wide expression profiles. Proc Natl Acad Sci 102:15545-15550, 2005
32. Orenbuch R, Filip I, Comito D, et al: arcasHLA: High-resolution HLA typing from RNAseq. Bioinformatics 36:33-40, 2020
33. Varghese AM, Singh I, Singh R, et al: Early-onset pancreas cancer: Clinical descriptors, genomics, and outcomes. J Natl Cancer Inst 113:1194-1202, 2021
34. Lowery MA, Jordan EJ, Basturk O, et al: Real-time genomic profiling of pancreatic ductal adenocarcinoma: Potential actionability and correlation with clinical phenotype. Clin Cancer Res 23: 6094-6100, 2017
35. Luo J: KRAS mutation in pancreatic cancer. Semin Oncol 48:10-18, 2021
36. Hallin J, Bowcut V, Calinisan A, et al: Anti-tumor efficacy of a potent and selective non-covalent KRAS(G12D) inhibitor. Nat Med 28:2171-2182, 2022
37. Guo R, Luo J, Chang J, et al: MET-dependent solid tumours—Molecular diagnosis and targeted therapy. Nat Rev Clin Oncol 17:569-587, 2020
38. Laskin J, Liu SV, Tolba K, et al: NRG1 fusion-driven tumors: Biology, detection, and the therapeutic role of afatinib and other ErbB-targeting agents. Ann Oncol 31:1693-1703, 2020
39. Proietti I, Skroza N, Michelini S, et al: BRAF inhibitors: Molecular targeting and immunomodulatory actions. Cancers (Basel) 12:1823, 2020
40. Chi J, Chung SY, Parakrama R, et al: The role of PARP inhibitors in BRCA mutated pancreatic cancer. Therap Adv Gastroenterol 14:175628482110148, 2021
41. Feng L, Qi Q, Wang P, et al: Serum levels of IL-6, IL-8, and IL-10 are indicators of prognosis in pancreatic cancer. J Int Med Res 46:5228-5236, 2018
42. Yu JH, Kim H: Role of janus kinase/signal transducers and activators of transcription in the pathogenesis of pancreatitis and pancreatic cancer. Gut Liver 6:417-422, 2012
43. Yang J, Yan J, Liu B: Targeting VEGF/VEGFR to modulate antitumor immunity. Front Immunol 9:978, 2018
44. Pagliuca S, Gurnari C, Rubio MT, et al: Individual HLA heterogeneity and its implications for cellular immune evasion in cancer and beyond. Front Immunol 13:944872, 2022
45. Zhao X, Zhang Y, Gao Z, et al: Prognostic value of peripheral © CD8(+) T cells in oligometastatic non-small-cell lung cancer. Future Oncol 18:55-65, 2022
46. Datta J, Bianchi A, De Castro Silva I, et al: Distinct mechanisms of innate and adaptive immune regulation underlie poor oncologic outcomes associated with KRAS-TP53 co-alteration in pancreatic cancer. Oncogene 41:3640-3654, 2022

APPENDIX

TABLE A1. Molecular Alterations in YOPC and AOPC

Pathway	Biomarker (mutation, CNA, or fusion)	Positive (AOPC)	Negative (AOPC)	Percentage (AOPC), %	Positive (YOPC)	Negative (YOPC)	Percentage (YOPC), %	*P*	*Q*
RTK/RAS	NGS-KRAS	1,749	176	90.9	221	51	81.3	**1.10E-06**	**.004**
	CNA-EGFR	1	1,914	0.1	2	268	0.7	.004	1
	NGS-RET	0	1,951	0.0	1	276	0.4	.008	1
TGF-β	CNA-SMAD2	0	1,893	0.0	1	266	0.4	.008	1
	NGS-SMAD4	391	1,553	20.1	40	233	14.7	.033	1
WNT	NGS-CTNNB1	16	1,934	0.8	9	267	3.3	.0003	.704
	NGS-RNF43	123	1,832	6.3	7	270	2.5	.012	1
Cell cycle	CNA-CDK6	16	1,881	0.8	7	261	2.6	.008	1
	NGS-CDKN2A	472	1,435	24.8	52	219	19.2	.045	1
Chromatin remodeling	NGS-SMARCB1	2	1,953	0.1	3	275	1.1	.001	.992
	CNA-SMARCB1	1	1,916	0.1	2	269	0.7	.004	1
Hedgehog	NGS-SMO	0	1,952	0.0	1	276	0.4	.008	1
Homologous recombination	NGS-BRCA2	41	1,894	2.1	13	262	4.7	.008	1
	NGS-PALB2	9	1,943	0.5	4	272	1.4	.044	1
MMR	NGS-MLH1	2	1,949	0.1	4	272	1.4	5.34E-05	.185
mRNA splicing	NGS-SF3B1	53	1,885	2.7	2	272	0.7	.046	1
PI3K	NGS-TSC1	0	1,952	0.0	2	275	0.7	.0002	.484
	NGS-MTOR	0	1,947	0.0	1	275	0.4	.008	1
	CNA-PIK3R2	0	791	0.0	1	126	0.8	.013	1
Others	CNA-KIF5B	0	1,827	0.0	2	258	0.8	.0002	.492
	NGS-JAK1	2	1,925	0.1	3	271	1.1	.001	.992
	NGS-TMEM127	0	1,133	0.0	1	143	0.7	.005	1
	CNA-TRIM27	0	1,912	0.0	1	268	0.4	.008	1
	CNA-EPHA3	0	1,870	0.0	1	263	0.4	.008	1
	CNA-IL7R	0	1,908	0.0	1	269	0.4	.008	1
	CNA-RALGDS	0	679	0.0	1	101	1.0	.010	1
	CNA-MLLT1	0	773	0.0	1	124	0.8	.013	1
	CNA-ELL	0	763	0.0	1	123	0.8	.013	1
	NGS-PRKAR1A	2	1,938	0.1	2	272	0.7	.022	1
	CNA-RARA	4	794	0.5	3	124	2.4	.025	1
	CNA-PRDM16	2	736	0.3	2	112	1.8	.031	1
	NGS-EPHA2	3	1,098	0.3	2	136	1.4	.040	1

NOTE. Numbers of positive and negative cases and overall percentages for top pathogenic gene mutations, fusions, and CNA are shown. All genes shown displayed differences with $P < .05$ (chi-square or Fisher's exact test). FDR-corrected $Q < .05$ is given in bold.

Abbreviations: AOPC, average-onset pancreatic cancer; CNA, copy number alterations; FDR, false discovery rate; MMR, mismatch repair; PI3K, phosphatidylinositol 3-kinase; YOPC, young-onset pancreatic cancer.

TABLE A2. List of Differentially Expressed Genes Between YOPC and AOPC

Gene	Age ≥70 Years	Age <70 Years	*P*	Fold Change	Log_2 Fold Change	*Q*
FGB	213.0639	253.103	5.35E-06	0.841807	−0.24844	.000262
CPB2	10.73488	13.16266	4.15E-06	0.815556	−0.29415	.000262
FGA	180.9031	213.5293	2.06E-05	0.847205	−0.23922	.000673
PLG	31.45159	38.41664	5.28E-05	0.818697	−0.2886	.001035
FGG	241.6043	282.0574	4.47E-05	0.856579	−0.22334	.001035
F2	9.288775	11.4822	9.46E-05	0.808971	−0.30584	.001545
F9	5.103183	5.930754	.000409	0.860461	−0.21682	.005722
SERPINB2	6.340134	5.738694	.001279	1.104804	0.143791	.014206
COL4A2	126.1337	135.8197	.001305	0.928685	−0.10674	.014206
DKK2	3.452056	3.712034	.00197	0.929963	−0.10475	.019308
IGFBP1	4.473332	5.262762	.004129	0.849997	−0.23447	.03679
IFNG	0.508028	0.480253	.005681	1.057833	0.081112	.046391
COL4A1	120.7089	129.6466	.007841	0.931061	−0.10305	.059106
F13A1	33.13304	31.58468	.014657	1.049023	0.069046	.095758
IL11	0.351676	0.368394	.01427	0.954619	−0.067	.095758
GUCY1A2	5.86866	6.169325	.02413	0.951265	−0.07208	.147794
SST	17.46769	15.94985	.033801	1.095163	0.131146	.194852
IGFALS	1.412191	1.541967	.035902	0.915837	−0.12684	.195464
F11	5.20928	5.966597	.041148	0.873074	−0.19582	.212236
SERPINE1	30.60093	32.15194	.045225	0.95176	−0.07133	.221602
COL4A5	5.343238	5.511835	.063907	0.969412	−0.04482	.272419
ADCY1	0.934538	0.904675	.063935	1.03301	0.046854	.272419
IFNA1	1.900172	1.645373	.058477	1.154858	0.207716	.272419
IGFBP3	35.88824	37.81646	.06762	0.949011	−0.0755	.276114
F2R	17.8615	18.57053	.071365	0.96182	−0.05616	.27975
GHRH	0.133716	0.117468	.075471	1.138313	0.186897	.284467
IL7	4.766534	4.597941	.082626	1.036667	0.051953	.299903
HLA-DRB3	11.7147	12.42623	.103898	0.94274	−0.08507	.363642
IGFBP6	9.694764	9.706376	.119517	0.998804	−0.00173	.390422
DKK1	22.10085	22.91794	.118374	0.964347	−0.05238	.390422
NOS3	6.61765	6.748245	.131233	0.980648	−0.02819	.403521
TRPC4	2.317167	2.436718	.134398	0.950938	−0.07258	.403521
TRPC5	0.240457	0.234866	.13588	1.023803	0.033938	.403521
IL3	0.040412	0.048445	.153974	0.834189	−0.26155	.443809
THY1	250.0147	256.8635	.158908	0.973337	−0.03899	.444942
KREMEN2	0.66296	0.714977	.163883	0.927246	−0.10898	.446127
CCR3	1.093817	1.05404	.177757	1.037737	0.053441	.470815
HLA-DRA	240.3654	232.0491	.201984	1.035839	0.050799	.520906
FZD1	5.426793	5.19561	.212446	1.044496	0.062807	.533839
KCNQ2	0.616584	0.676582	.217989	0.911322	−0.13397	.534073
IGFBP5	139.5291	142.7088	.253947	0.977719	−0.03251	.606994
WNT8B	0.196908	0.187153	.266235	1.052122	0.073302	.621216
GHRL	1.549805	1.969712	.275682	0.786818	−0.3459	.628299
IL1B	9.159799	8.311716	.28624	1.102035	0.14017	.637535
RAPGEF5	22.38004	23.16832	.320002	0.965976	−0.04994	.640003
PLAU	13.92074	14.346	.301644	0.970357	−0.04341	.640003
CD3D	10.69667	11.29104	.302337	0.947359	−0.07802	.640003
IGF1	5.536212	5.559563	.308441	0.9958	−0.00607	.640003
EPO	0.189023	0.208045	.319003	0.908568	−0.13833	.640003
ITGB2	80.68734	76.83119	.330846	1.05019	0.07065	.648459

(continued on following page)

TABLE A2. List of Differentially Expressed Genes Between YOPC and AOPC (continued)

Gene	Age ≥70 Years	Age <70 Years	*P*	Fold Change	Log_2 Fold Change	*Q*
ITGAX	16.62007	15.83322	.343258	1.049696	0.069971	.659594
IGFBP4	42.73864	43.66044	.370802	0.978887	−0.03079	.661693
ITGAL	15.41324	15.15506	.371358	1.017036	0.024371	.661693
COL4A6	0.729051	0.737712	.369763	0.98826	−0.01704	.661693
PLAT	132.5589	130.0715	.367849	1.019123	0.027329	.661693
CD8A	3.415586	3.407509	.404158	1.00237	0.003415	.707277
CCL11	2.96355	3.101497	.424294	0.955523	−0.06564	.729488
APP	279.2316	283.0418	.44122	0.986538	−0.01955	.74551
CD28	3.54859	3.457023	.480784	1.026487	0.037716	.76157
CD4	8.300176	8.062119	.463251	1.029528	0.041983	.76157
IL2	0.266584	0.279494	.479105	0.953809	−0.06823	.76157
TLR7	2.848408	2.722911	.482509	1.046089	0.065006	.76157
ANPEP	55.2169	48.97576	.489581	1.127433	0.173042	.76157
HLA-DRB5	33.96501	35.24904	.510114	0.963573	−0.05353	.781112
PTPRC	0.345803	0.348093	.55971	0.99342	−0.00952	.818681
GNAS	190.484	192.1411	.555008	0.991376	−0.0125	.818681
COL4A3	2.246328	2.306565	.558027	0.973884	−0.03818	.818681
CD5	3.249027	3.293036	.579605	0.986636	−0.01941	.835313
IL10	1.410248	1.284904	.615607	1.097551	0.134288	.86185
HLA-DRB1	134.2702	131.7672	.607662	1.018996	0.027148	.86185
CSF1	15.09522	14.63318	.635041	1.031574	0.044848	.876536
COL4A4	1.664774	1.619377	.645554	1.028033	0.039887	.878671
IL13	0.148691	0.166913	.658406	0.890831	−0.16678	.883887
CSF3	0.241441	0.270488	.669021	0.892615	−0.16389	.886001
CD3E	3.611179	3.676768	.679651	0.982161	−0.02597	.888077
WNT8A	0.212926	0.210431	.699022	1.011857	0.017005	.901371
GUCY1B2	0.117637	0.114455	.721064	1.027805	0.039567	.916251
IL5RA	0.5349	0.525738	.738611	1.017426	0.024924	.916251
CSF2	0.464305	0.490354	.736615	0.946876	−0.07875	.916251
KCNQ4	1.031623	1.061972	.7602	0.971422	−0.04183	.925889
CD33	2.685025	2.571431	.765276	1.044175	0.062364	.925889
CD40	6.996738	7.014987	.785324	0.997399	−0.00376	.92725
IFNB1	0.40215	0.398549	.784699	1.009034	0.012974	.92725
KCNQ5	1.984083	2.036391	.81366	0.974313	−0.03754	.938102
IL5	0.918246	0.891812	.81098	1.029641	0.042142	.938102
GH1	0.253986	0.240908	.879246	1.054285	0.076265	.94375
CD247	1.340309	1.352437	.894933	0.991033	−0.013	.94375
CD3G	2.645035	2.61187	.898651	1.012698	0.018204	.94375
CD2	5.977274	5.972806	.843204	1.000748	0.001079	.94375
TRPC3	0.60144	0.585058	.876152	1.028	0.03984	.94375
ICAM1	17.30879	17.27843	.863639	1.001757	0.002533	.94375
CD7	2.710846	2.767003	.837295	0.979705	−0.02958	.94375
TRPV4	9.437347	9.389004	.905229	1.005149	0.007409	.94375
IL6	2.973981	2.991521	.857324	0.994137	−0.00848	.94375
IL9	0.120191	0.108006	.944594	1.112816	0.154215	.954332
IL4	0.571577	0.553736	.939582	1.032219	0.045749	.954332
KCNQ3	1.195197	1.204244	.939356	0.992487	−0.01088	.954332
IGFBP2	19.61493	20.58527	.985116	0.952862	−0.06966	.985116

NOTE. Genes are listed in order of statistical significance (*Q* value).
Abbreviations: AOPC, average-onset pancreatic cancer; YOPC, young-onset pancreatic cancer.

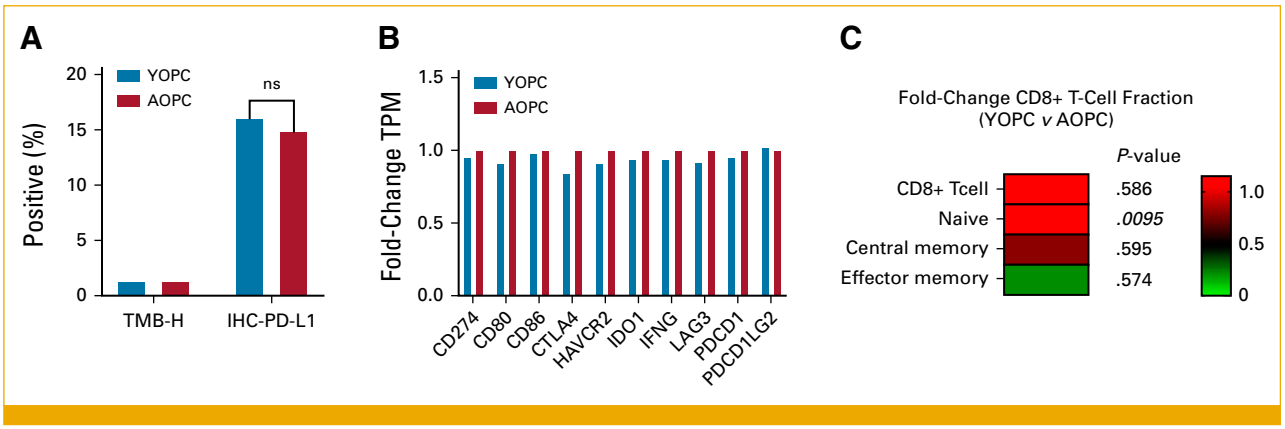

FIG A1. Immune landscape of YOPC and AOPC. (A) Percentage of cases positive for immunotherapy biomarkers TMB-H and PD-L1(+) for YOPC (blue bars, n = 273-292 [a small number of patients lacked PD-L1 IHC or dMMR/MSI-H analysis]) and AOPC (red bars, n = 2,028-2,138 [a small number of patients lacked PD-L1 IHC or dMMR/MSI-H data]). Statistical analysis was performed using the chi-square or Fisher's exact test. (B) Fold-change gene expression levels in TPM of immune checkpoint genes between YOPC (blue bars, n = 284) and AOPC (red bars, n = 2,089). AOPC expression is set to 1 for each gene. There were no statistically significant differences in immune gene expression between YOPC and APOC (determined using the Mann-Whitney U test). (C) Fold-change median $CD8^+$ T-cell fractions (YOPC *v* AOPC) calculated by xCell immune deconvolution. *P* value determined using the Kruskal-Wallis test. Significant *P* value (<.05) indicated by italics. AOPC, average-onset pancreatic cancer; dMMR, mismatch repair deficiency; IHC, immunohistochemistry; MSI-H, microsatellite instability-high; TMB-H, tumor mutational burden-high; TPM, transcripts per million; YOPC, young-onset pancreatic cancer.